Using the Torso to Compensate for Non-Minimum Phase Behaviour in ZMP Bipedal Walking

Houman Dallali, Martin Brown, and Bram Vanderborght

Abstract. In Zero Moment Point (ZMP) bipedal walking, the conventional method is to use the cart-table model for generating the reference trajectory [1]. However, due to modeling and tracking errors and external disturbances, such as uneven terrain, the generated trajectory must be adapted by a stabilizer that uses sensory inputs from force and torque sensors placed in the robot's feet. The problem with the cart-table model is that it is non-minimum phase which causes a significant, undesirable undershoot in the ZMP in order to cancel the effect of disturbances. In this paper, a novel scheme is proposed for ZMP feedback stabilization that utilizes the upper body to balance the humanoid robot. This method increases the performance and robustness of walking by reducing the undershoot and maintaining a desired bandwidth. The effectiveness of the proposed scheme is demonstrated using simulation and open problems are discussed.

1 Introduction

A current and interesting robotics research area is walking bipedal robots. Studying bipedal robots introduces interdisciplinary challenges in applied mathematics, mechanical, computer and control engineering. During the past two decades, significant advances have been made in this area and current bipedal robots are capable of walking in well structured environments, on flat and sloped terrains [2],[3],[4],[5].

Houman Dallali · Martin Brown
The University of Manchester, Control Systems Centre, School of Electrical and Electronic Engineering, M60 1QD, United Kingdom,
e-mail: houman.dallali@postgrad.manchester.ac.uk, martin.brown@manchester.ac.uk

Bram Vanderborght
Italian Institute of Technology, Robotics, Brain and Cognitive Sciences Department, Via Morego 30, 16163 Genova, Italy,
e-mail: bram.vanderborght@iit.it

In bipedal locomotion, cyclic walkers have been a focus of recent attention. This consists of energy shaping approaches which are based on nonlinear control theory [6],[7] and hybrid control approaches based on the notion of virtual constraints [8]. However, both approaches have only been implemented for 2D robots and the extensions to 3D is still under study. In addition, versatility, where a robot walks on discrete footholds and to turn or change its limb coordination, is an integral part of locomotion that can not be achieved using a cyclic walking approach. One practical scheme to control humanoid robots is based on the concept of Zero Moment Point (ZMP)[9]. ZMP is defined as the point on the ground plane about which the total moments due to ground contact forces become zero. For stability the ZMP must always reside in the convex hull of the ground contact points. In order to satisfy this criterion, [10] considered the non-minimum phase problem of balancing and proposed a nonlinear invariant control approach for planar robots. A conventional ZMP based trajectory generation method that can be implemented in 3D is the cart-table model that approximates the dynamics of a bipedal robot by a running cart on a pedestal table which is a linear and intuitive model [1]. It should be noted that the robots that fit in this scheme must be fully actuated and position controlled.

Due to the modeling and tracking errors, external disturbances such as the ground type and unknown external forces the actual ZMP trajectory will be different from the desired reference trajectory. The actual ZMP trajectory is obtained from measurements, such as force and torque sensors placed on the foot. The deviation of the actual ZMP trajectory from the desired reference trajectory has to be tracked by a controller (stabilizer) to generate the required change in the joint torques. However, these deviations can be large enough to destabilize the robot. HRP-1S can perform stable walking in simulation, but falls in practice [12]. The addition of a feedback stabilizer means that robot is also able to walk in experiments because it is able to cope with (limited) unknown disturbances. The tracking of the desired horizontal motion of Johnnie is suspended whenever the ZMP approaches an instability region [13]. However, the cart-table model is non-minimum phase and hence the stabilizers will have limited tracking performance of such errors, in terms of the bandwidth and the amount of undershoot

In this paper, an overview of the cart-table model for ZMP trajectory generation and its non minimum phase behaviour is given in section 2 and a two mass inverted pendulum is introduced to model the robot's upper body and introduce actuation in the hip. In section 3 these two models are combined to solve the non-minimum phase behaviour of the cart-table model, by including an upper body model. The dynamic performance is analyzed theoretically and in section 3.2, and an LQR optimal controller is formulated for the new multi-variable system to generate the reference walking trajectories. In section 3.3 a ZMP stabilizer is proposed to use the torso in balancing the robot. Finally, the effectiveness of the proposed scheme is evaluated by simulation and open problems are discussed.

2 Literature Review

In this section, an overview of the cart-table trajectory generation model is provided. This includes analyzing the model's unstable zero which causes the non-minimum

phase behaviour and discussing the implications for control design. Next, a simple two mass inverted pendulum model of the robot's hip and torso is reviewed, and its benefits and limitations are mentioned [17]. This is to motivate the combination of the two models in section 3.2.

2.1 Linear Inverted Pendulum and Cart-Table Model

In [14] a 3D linear inverted pendulum model for bipedal walking trajectory generation was introduced. The 3D inverted pendulum is constrained to move along a plane which results in linear state space equations as illustrated in figure 1. In [1] it was shown that this directly corresponds to the dynamics of a running cart on a pedestal table and the cart-table dynamics are:

$$\begin{aligned} p_x &= x - \tfrac{z_c}{g}\ddot{x} \\ p_y &= y - \tfrac{z_c}{g}\ddot{y} \end{aligned} \tag{1}$$

where p_x,p_y are the zero moment points in X and Y directions, respectively, z_c is the height of the cart and g is gravity. In this paper, the problem is studied in the frontal plane (i.e. ZMP in X direction is considered) but under certain assumptions the motion in both frontal and lateral planes can be decoupled. Therefore, the models in this section and the proposed model in section 3 are also valid for 3D walking [14]. Equation 1 can be represented in state space form using a new variable u_x which is the time derivative of the horizontal acceleration (jerk) of center of mass, $\frac{d}{dt}\ddot{x} = u_x$:

$$\dot{\mathbf{x}} = \begin{bmatrix} 0 & 1 & 0 \\ 0 & 0 & 1 \\ 0 & 0 & 0 \end{bmatrix} \mathbf{x} + \begin{bmatrix} 0 \\ 0 \\ 1 \end{bmatrix} u_x \,, \quad p_x = [1 \quad 0 \quad \tfrac{-z_c}{g}]\mathbf{x} \tag{2}$$

where $\mathbf{x} = (x, \dot{x}, \ddot{x})^T$. The cart-table model provides a convenient framework to generate a reference trajectory for the bipedal robot. However, in ZMP feedback

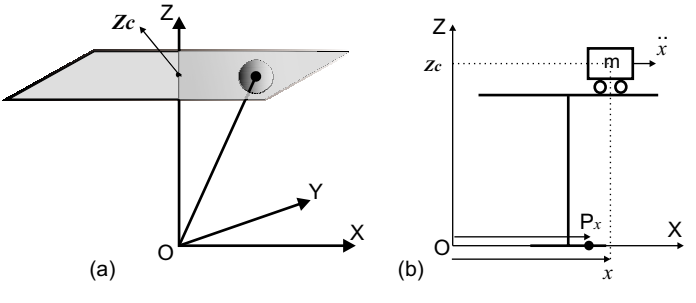

Fig. 1 In (a) constrained linear inverted pendulum is shown that assumes that ZMP is in the origin (0,0,0) (origin corresponds to the robot's ankle) and the ankle torque is zero. In (b) the cart-table model is shown for ZX (frontal) plane where the ZMP can move in the foot (table's contact with the ground) and the ankle's torque is not necessarily zero.

stabilization a problem arises from the non-minimum phase behaviour of equation 2. The transfer function of the equation 2 is:

$$G(s) = \frac{p_x(s)}{u_x(s)} = \frac{1 - (\frac{-z_c}{g})s^2}{s^3} = \left(\frac{-z_c}{g}\right)\frac{(\frac{-g}{z_c}) - s^2}{s^3} \tag{3}$$

This is unstable because it has three poles at the origin (triple integrator) but this can be overcome using pole placement. However, equation 3 also has two zeros. Using feedback will not affect the positions of the zeros and this will cause problems in the control design. The left half plane zero has a scaling effect on the response which can be solved by dc gain adjustment, but the right half plane zero will limit the achievable bandwidth of the system and produces an undesirable undershoot [15] as the inverse is unstable. For ZMP feedback stabilization, consider the case where the desired ZMP is in front of the actual ZMP of the robot. The hip must accelerate in the positive direction and according to equation 2 the ZMP will initially move backward and hence diverge as illustrated in figure 2. Therefore, it is important to investigate methods for minimizing/overcoming this behaviour in order to increase the robustness to disturbances such as uneven surfaces.

In general, perfect tracking control of such systems without future information of the tracking signal is not possible and it is necessary to approximate the non-minimum phase system with a minimum phase system to design controllers with bounded tracking error [16]. In addition, controller design based on right half plane pole-zero cancelation is fundamentally flawed, due to the loss of internal stability as such designs rely on unstable pre-filters. Therefore, performance limitations, due to the right half plane zeros, will be present in any design leading to inevitable compromises between the speed of response and the amount of undershoot in the system's step response. In figure 2 this is shown for the cart-table model which is stabilized using pole-placement.

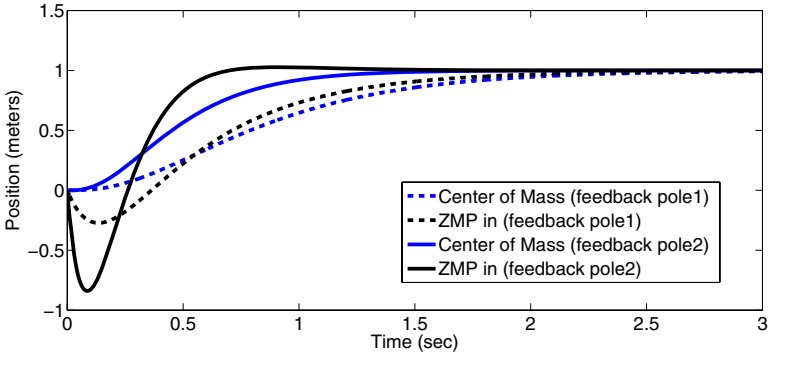

Fig. 2 Cart-table model step response with poles placed at pole1=[-2,-4,-6], pole2=[-4,-6,-10]. In the first case (dotted line) the ZMP rise time is 1.04s and ZMP undershoot is 27% (notice the slow response of center of mass) while in the second case (solid line) the ZMP rise time is 0.275s and ZMP undershoot is 84% (in this case the center of mass quickly approaches the steady state). This shows the trade off in bandwidth and undershoot criteria.

2.2 Two Mass Inverted Pendulum Model

The non-minimum phase problem of one-mass inverted pendulum model which represents the center of mass of a robot was first analyzed in [17] and a two mass inverted pendulum was proposed that results in a multi-variable minimum phase system, as illustrated in figure 3. Linearization about the origin produces the following state space equations:

$$\begin{gathered}\dot{\mathbf{x}} = \begin{bmatrix} 0 & I_{2\times 2} \\ 0 & 0 \end{bmatrix} \mathbf{x} + \begin{bmatrix} 0 \\ I_{2\times 2} \end{bmatrix} \mathbf{u}\,, \quad p_x = [c_1\ c_2\ 0\ 0]\mathbf{x} + [d_1\ d_2]\ \mathbf{u} \\ c_1 = \frac{(m_1+m_2)l_1+m_2l_2}{m_1+m_2}\,,\ c_2 = \frac{m_2l_2}{m_1+m_2}\,,\ d_1 = -\frac{m_1l_1^2+m_2(l_1+l_2)^2}{(m_1+m_2)g}\,,\ d_2 = -\frac{m_2(l_1+l_2)l_2}{(m_1+m_2)g}\end{gathered} \tag{4}$$

where $\mathbf{x} = (\theta_1, \theta_2, \dot{\theta}_1, \dot{\theta}_2)^T$ and $\mathbf{u} = (u_1, u_2)^T = (\ddot{\theta}_1, \ddot{\theta}_2)^T$ and p_x are the input vector and scalar output of the two mass inverted pendulum, respectively. It can be shown that this has no right half plane zeros provided the second link's length is non-zero. The transfer function matrix of two mass inverted pendulum can be obtained as following:

$$G(s) = C(sI - A)^{-1}B + D = [\frac{c_1 + d_1s^2}{s^2} \quad \frac{c_2 + d_2s^2}{s^2}] \tag{5}$$

It should be noted that the zeros in multi-variable systems are different from their SISO counterparts, and they are associated with the directions of input and output of the system. To obtain the zeros of equation 5, the transfer function, $G(s)$, is epxressed as:

$$G(s) = \frac{\Pi(s)}{D_G(s)}\,, \quad \Pi(s) = [c_1 + d_1s^2 \quad c_2 + d_2s^2]\,, \quad D_G(s) = s^2 \tag{6}$$

The roots of greatest common divisor of $\Pi(s)$ determines the zeros of the transfer function matrix $G(s)$, which in this case does not have a root.

Therefore, the transfer function does not have any zeros and hence the double inverted pendulum is minimum phase. However, as mentioned earlier, this scheme has limitations due to the linearization of the two masses around the vertical line. This can produce large errors as the robot's hip is required to move in a large operating range that cannot be approximated by linearizing about a single operating

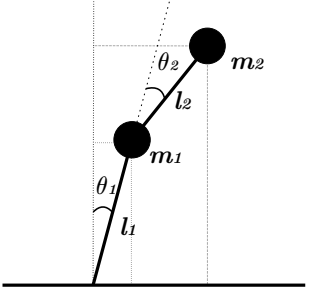

Fig. 3 The two mass inverted pendulum model relies on linearization of both upper and lower pendulum links. This is not the case for the robot as the motion of the hip is completely nonlinear and it can lead to large modeling errors for the trajectory generation.

point [11]. In addition, the inverted pendulum models assume ZMP in the ankle and ankle torque is zero, while in the cart-table model, the ZMP is located in the foot and ankle torque is not necessarily zero. In section 3, a new model is proposed that combines the advantages of cart-table model and two mass inverted pendulum.

3 Generalized Two Link Inverted Pendulum

In this section firstly a new model is proposed which combines the advantages of the cart-table and the two mass inverted pendulum models. The new model does not assume linearization of the lower mass that corresponds to the robot's hip motion. Secondly, a trajectory generation for the model based on preview control of ZMP is described in section 3.2 . Thirdly, a solution to ZMP stabilization is proposed in section 3.3.

3.1 Modeling

Consider the pendulum-cart-table model shown in figure 4. The equation for torques around the ZMP gives:

$$\tau_{zmp} = -Mg(x - p_x) + M\ddot{x}z_c - (mg + m\ddot{z}_2)(x_2 - p_x) + m\ddot{x}_2(z_c + z_2) = 0 \quad (7)$$

where $z_2 = l\cos(\theta)$, $x_2 = x + l\sin(\theta)$, and l is the pendulum's length. . Assuming small deviation on the torso and linearizing around the vertical axis where $z_2 = l$ and $x_2 = x + l\theta$, this results in the following linear relationship:

$$p_x = x + \frac{ml}{(M+m)}\theta - \frac{Mz_c + m(z_c + l)}{(M+m)g}\ddot{x} - \frac{ml(z_c + l)}{(M+m)g}\ddot{\theta} = (1, c_1, 0, 0, c_2, c_3)\mathbf{x} \quad (8)$$

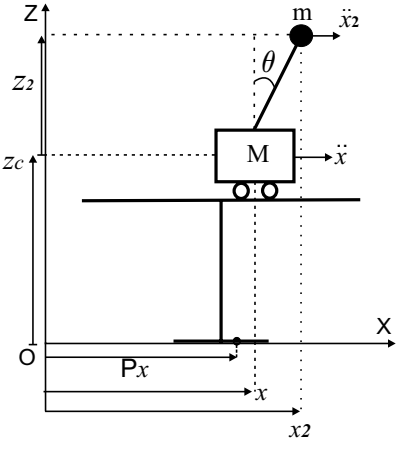

Fig. 4 The new pendulum-cart-table model in 2D. The cart represents the hip and the actuated pendulum represents the torso.

where $\mathbf{x} = (x, \theta, \dot{x}, \dot{\theta}, \ddot{x}, \ddot{\theta})^T$ is the state vector and the control input vector is $\mathbf{u} = (u_1, u_2)^T$ where $u_1 = \frac{d}{dt}\ddot{x}$ and $u_2 = \frac{d}{dt}\ddot{\theta}$. Therefore, the system for control of ZMP can be defined as:

$$\dot{\mathbf{x}} = \begin{bmatrix} 0 & I_{4\times 4} \\ 0 & 0 \end{bmatrix} \mathbf{x} + \begin{bmatrix} 0 \\ I_{2\times 2} \end{bmatrix} \mathbf{u}\,, \quad y = p_x = \begin{bmatrix} 1 & c_1 & 0 & 0 & c_2 & c_3 \end{bmatrix} \mathbf{x} \tag{9}$$

The transfer function matrix for this system is given by:

$$G(s) = C(sI - A)^{-1}B = \frac{1}{s^3}\begin{bmatrix} 1 + c_1 s^2 & c_2 + c_3 s^2 \end{bmatrix} \tag{10}$$

and in a similar fashion to section 2.2 the system does not have any zeros. Therefore, one can design a multi-variable controller to achieve the desired bandwidth required for the purpose of feedback stabilization.

3.2 Trajectory Generation Using Preview Control of ZMP

Consider the dynamics of pendulum-cart-table model given by equation 9. The discrete time dynamics can be expressed by:

$$\mathbf{x}(k+1) \;=\; A\mathbf{x}(k) \;+\; B\,\mathbf{u}(k), \qquad \mathbf{y}(k) \;=\; C\mathbf{x}(k) \tag{11}$$

where $\mathbf{x}(k) = (x(k), \theta(k), \dot{x}(k), \dot{\theta}(k), \ddot{x}(k), \ddot{\theta}(k))^T$, $\mathbf{u}(k) = (u_1(k) \;\; u_2(k))^T$ and A, B are the discrete time versions of equation 9 with sample time T. To add robustness to the control, integral action is introduced by using incremental control, $\Delta\mathbf{u}(k) = \mathbf{u}(k) - \mathbf{u}(k-1)$, and state, $\Delta\mathbf{x}(k) = \mathbf{x}(k) - \mathbf{x}(k-1)$, [19]. The state vector is augmented as $\tilde{\mathbf{x}}(k) = (p_x(k), \Delta\mathbf{x}(k))^T$ and the dynamics now become:

$$\tilde{A} = \begin{bmatrix} I & CA \\ 0 & A \end{bmatrix} \quad \tilde{B} = \begin{bmatrix} CB \\ B \end{bmatrix} \quad \tilde{C} = \begin{bmatrix} 1 & \mathbf{0}_{1\times 6} \end{bmatrix} \tag{12}$$

An optimal control problem is formulated by minimizing:

$$J = \sum_{i=k}^{\infty} [e^T(i) Q_e e(i) + \Delta\mathbf{x}^T(i) Q_x \Delta\mathbf{x}(i) + \Delta\mathbf{u}^T(i) R \Delta\mathbf{u}(i)] \tag{13}$$

where $e(i) = p_x(i) - p_{ref}(i)$, and the optimal control is given by [19]:

$$u^o(k) \;=\; -G_I \sum_{i=0}^{k} e(k) \;-\; G_x x(k) - \sum_{i=1}^{NL} G_d(i) p_{ref}(k+i) \tag{14}$$

where p_{ref} is the reference ZMP trajectory in x direction. The parameter N_L determines the horizon of the future desired ZMP. The optimal gain is determined by solving the discrete time algebraic Riccati equation:

$$\tilde{P} = \tilde{A}^T \tilde{P} \tilde{A} - \tilde{A}^T \tilde{P} \tilde{B} (R + \tilde{B}^T \tilde{P} \tilde{B})^{-1} \tilde{B}^T \tilde{P} \tilde{A} + \tilde{Q} \tag{15}$$

where, $\tilde{Q} = diag\{Q_e, Q_x\}$. Hence the optimal gain is defined by:

$$\tilde{K} = [G_I \quad G_x] \;=\; (R + \tilde{B}^T \tilde{P} \tilde{B})^{-1} \tilde{B}^T \tilde{P} \tilde{A} \tag{16}$$

and the optimal preview gain is calculated using the recursive formula:

$$\begin{aligned} G_d(l) &= (R + \tilde{B}^T \tilde{P} \tilde{B})^{-1} \tilde{B}^T \tilde{X}(l-1), \\ \tilde{X}(l) &= \tilde{A_c}^T \tilde{X}(l-1), \quad l = 2, ..., N_L, \end{aligned} \tag{17}$$

where $\tilde{A_c} = \tilde{A} - \tilde{B}\tilde{K}$, $G_d(1) = G_I$ and $\tilde{X}(1) = -\tilde{A_c}^T \tilde{P}[1 \quad \mathbf{0}_{1\times 6}]^T$. A numerical example is given in the section 4 where the generator is producing the desired motion of center of mass. In the next section, the stabilization issue associated with ZMP based walking is considered.

3.3 Stabilizer Design

In section 3.2, a walking reference trajectory generator based on the new pendulum-cart-table model was introduced. However, due to imperfect ground conditions, modeling errors and unknown disturbances, a real time feedback stabilizer must be used to adapt the generated trajectories based on the sensor information. This section proposes a ZMP feedback stabilization scheme to increase the robustness in bipedal walking.

Consider equation 9 with outputs modified as:

$$\dot{\mathbf{x}} = \begin{bmatrix} 0 & I_{4\times 4} \\ 0 & 0 \end{bmatrix} \mathbf{x} + \begin{bmatrix} 0 \\ I_{2\times 2} \end{bmatrix} \mathbf{u}\,, \quad \mathbf{y} = \begin{bmatrix} p_1 \\ p_2 \end{bmatrix} = \begin{bmatrix} 1 & 0 & 0 & 0 & c_2 & 0 \\ 0 & c_1 & 0 & 0 & 0 & c_3 \end{bmatrix} \mathbf{x} \tag{18}$$

where p_1 and p_2 are the ZMP outputs corresponding to hip and torso, respectively. Reference tracking using feedback can then be implemented by considering the system defined in equation 18 in compact format as:

$$\dot{\mathbf{x}} = A\mathbf{x} + B\mathbf{u} \;\;,\;\; \mathbf{y} = C\mathbf{x} \tag{19}$$

Define the integral of error, $\mathbf{z}$, between reference vector $\mathbf{r}$ and the system's output vector $\mathbf{y}$, ie. $\dot{\mathbf{z}} = \mathbf{r} - \mathbf{y}$, then the new state space system is:

$$\begin{bmatrix} \dot{\mathbf{x}} \\ \dot{\mathbf{z}} \end{bmatrix} = \begin{bmatrix} A & 0 \\ -C & 0 \end{bmatrix} \begin{bmatrix} \mathbf{x} \\ \mathbf{z} \end{bmatrix} + \begin{bmatrix} B \\ 0 \end{bmatrix} \mathbf{u} + \begin{bmatrix} 0 \\ I \end{bmatrix} \mathbf{r} \;\;,\;\; \mathbf{y} = \begin{bmatrix} C & 0 \end{bmatrix} \begin{bmatrix} \mathbf{x} \\ \mathbf{z} \end{bmatrix} \tag{20}$$

Since the system in equation 20 is controllable, it is possible to use feedback $\mathbf{u} = -[K_1 \quad K_2]\mathbf{x}$ to stabilize the system and track the reference vector $\mathbf{r}$. As a result of feedback the closed loop system is:

$$\begin{bmatrix} \dot{\mathbf{x}} \\ \dot{\mathbf{z}} \end{bmatrix} = \begin{bmatrix} A - BK_1 & -BK_2 \\ -C & 0 \end{bmatrix} \begin{bmatrix} \mathbf{x} \\ \mathbf{z} \end{bmatrix} + \begin{bmatrix} 0 \\ I \end{bmatrix} \mathbf{r} \;\;,\;\; \mathbf{y} = \begin{bmatrix} C & 0 \end{bmatrix} \begin{bmatrix} \mathbf{x} \\ \mathbf{z} \end{bmatrix} \tag{21}$$

A numerical example for the ZMP stabilization is given in section 4 and the results are compared with the old cart-table model.

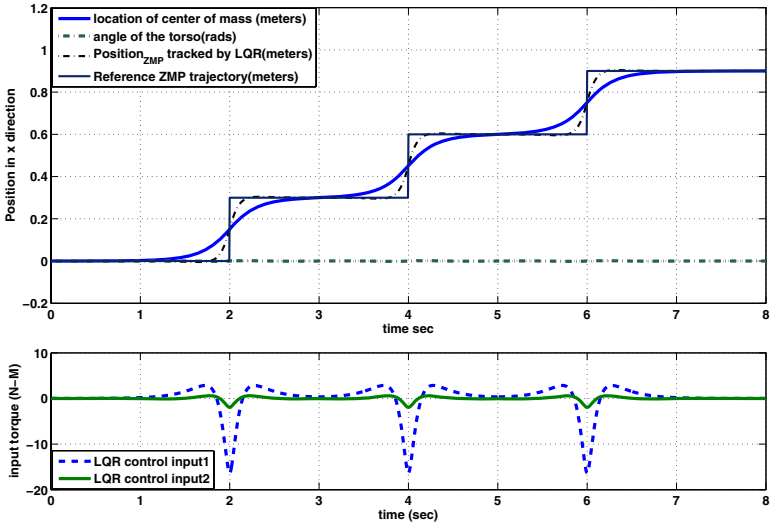

Fig. 5 An illustration of the reference ZMP trajectory generation using the new pendulum-cart-table model. The location of torso is kept in the vertical direction, however it can be moved depending on the ground slope. The control input signals are shown in the lower figure.

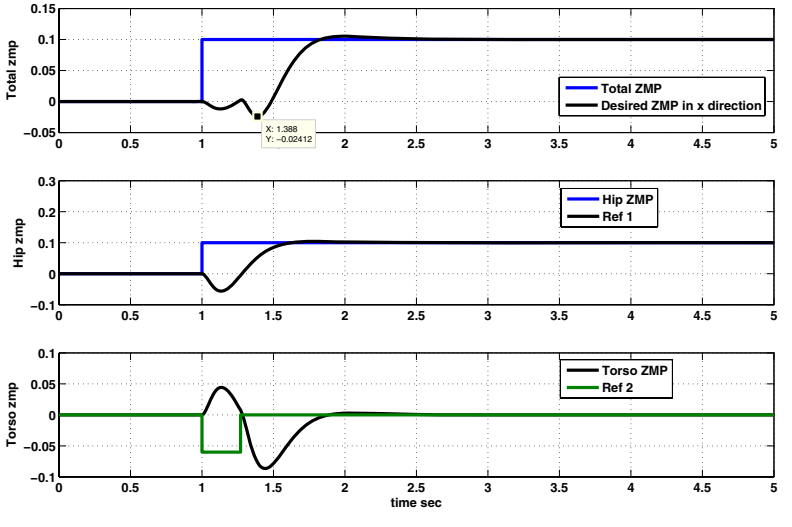

Fig. 6 An illustration of the use of torso in minimizing the amount of undershoot, for the purpose of stabilization and balancing.

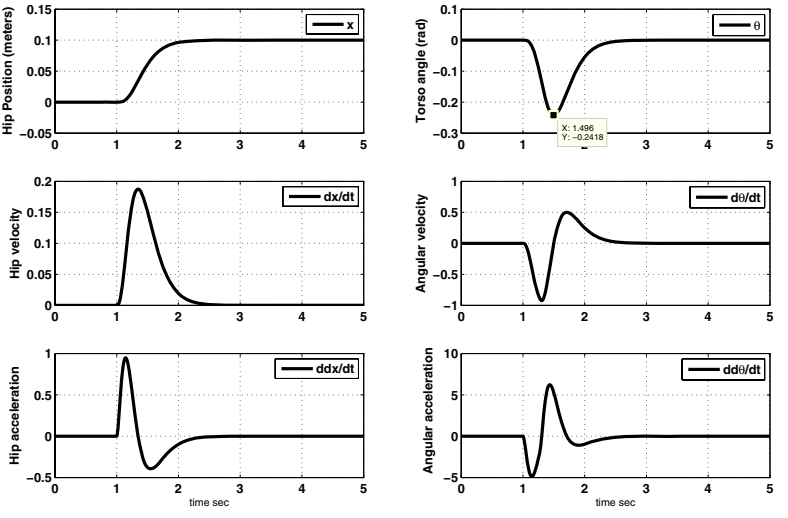

Fig. 7 An illustration of the state evolution in the pendulum-cart-table model. Note that the upper body is moving by maximum of 0.24rad.

4 Comparison and Simulation Results

In order to implement ZMP based walking, a stable trajectory of center of mass that satisfies the desired ZMP must be generated and during trajectory following a real time stabilization mechanism must be used to adapt the trajectories and react to unknown disturbances. Therefore, the results of this paper are two fold. Firstly, a numerical example is provided to illustrate the reference trajectory generation introduced in section 3.2. Simulation results of ZMP tracking and the location of center of mass (robot's hip) associated with the pendulum-cart-table model is given in figure 5, and the controller and model parameters are given as follows: $g = 9.81$, $z_c = 0.6m$, $m = 8Kg$, $M = 12.5Kg$, $l = 0.3m$, $T = 0.005s$; preview time $Tprev = 2s$, $Q_e = I_{2\times2}$, $Q_x = I_{6\times6}$, $R = 10^{-3} \times I_{2\times2}$ and the simulation time is $8sec$. Secondly, a numerical example of the real time feedback scheme that was introduced in section 3.3 is illustrated in figure 6. Note that the step height is 0.1 m and the system poles are placed at $[-6-6-8-8-10-10-12-12]$. The undershoot corresponding to the hip is reduced from 5.6cm to 2.4cm by using the upper body movement, which is a 57% reduction in the total ZMP of the new pendulum-cart-table model. At the same time the settling time in cart ZMP step response is 0.53s and in the total ZMP response the settling time is 0.74s. That is the new model can achieve a reasonable tracking speed, and avoid the undesired undershoot. In addition, due to practical limitations, the range of upper body movement must be as small as possible. This is achieved and demonstrated in figure 7.

5 Conclusions and Future Work

In this paper, the non-minimum phase problem associated with using the cart-table model for ZMP reference trajectory generation has been described and a solution has been proposed based on actuating the torso. The new pendulum-cart-table model combines the advantages of existing models and makes use of the torso to compensate the unknown ZMP deviations. The effectiveness of this model has been shown by numerical examples both for pattern generation and for ZMP feedback stabilization. In ZMP stabilization the torso is used for reducing or ideally canceling the undesired effects of undershoots and bandwidth limitations. However, this method can be used in combination with existing stabilization schemes that use ankle actuation. All the results mentioned in this paper are valid for the three dimensional case where the sagittal and lateral motions can be decoupled. The future, work should combine the ankle and torso actuation for the purpose of stabilization, as it can be observed in human walking.

Acknowledgements. This research has been done on the CICADA project which is financed by the EPSRC grant EP/E050441/1 and the University of Manchester. The authors would like to thank IIT and especially Prof D. Caldwell and Dr N. Tsagarakis for their support.

References

1. Kajita, S., Kanehiro, F., Kaneko, K., Fujiwara, K., Harada, K., Yokoi, K., Hirukawa, H.: Biped walking pattern generation by using preview control of zero-moment point. In: ICRA, vol. 2, pp. 1620–1626 (2003)
2. Kanehira, N., Kawasaki, T., Ohta, S., Ismumi, T., Kawada, T., Kanehiro, F., Kajita, S., Kaneko, K.: Design and experiments of advanced leg module (HRP-2L) for humanoid robot (HRP-2) development. In: IROS, vol. 3, pp. 2455–2460 (2002)
3. Sakagami, Y., Watanabe, R., Aoyama, C., Matsunaga, S., Higaki, N., Fujimura, K.: The intelligent ASIMO: system overview and integration. In: IEEE/RSJ IROS, vol. 3, pp. 2478–2483 (2002)
4. Vanderborght, B., Van Ham, R., Verrelst, B., Van Damme, M., Lefeber, D.: Overview of the Lucy-project: Dynamic stabilisation of a biped powered by pneumatic artificial muscles. Advanced Robotics 22(6-7) (10), 1027–1051 (25) (2008)
5. Pfeiffer, F., Lffler, K., Gienger, M.: The Concept of Jogging JOHNNIE. In: ICRA, vol. 3, pp. 3129–3135 (2002)
6. Holm, J.K., Spong, M.W.: Kinetic energy shaping for gait regulation of underactuated bipeds. In: Proceedings of the 17th IEEE International Conference on Control Applications, pp. 1232–1238 (2008)
7. Ames, A.D., Gregg, R.D., Spong, M.W.: A Geometric Approach to Three-Dimensional Hipped Bipedal Robotic Walking. In: 46th IEEE Conference on Decision and Control (2007)
8. Chevallereau, C., Abba, G., Aoustin, Y., Plestan, F., Westervelt, E., Canudas-de-Wit, C., Grizzle, J.W.: RABBIT: A testbed for advanced control theory. IEEE Control Systems Magazine 23(5), 57–79 (2003)

9. Vukobratovic, M., Juricic, D.: Contribution to the synthesis of biped gait. IEEE Trans. Biomed. Eng. BME-16(1), 1–6 (1969)
10. Sobotka, M., Wolff, J., Buss, M.: Invariance Controlled Balance of Legged Robots. In: European Control Conference (2007)
11. Kajita, S., Tani, K.: Study of Dynamic Biped Locomotion on Rugged Terrain- theory and basic experiment. In: ICAR, Robots in Unstructured Environments, vol. 1, pp. 741–746 (1991)
12. Hirukawa, H., Kanehiro, F., Kajita, S., Fujiwara, K., Yokoi, K., Kaneko, K., Harada, K.: Experimental evaluation of the dynamic simulation of biped walking of humanoid robots. In: ICRA, vol. 2, pp. 1640–1645 (2003)
13. Pfeiffer, F., Lffler, K., Gienger, M.: Humanoid robots. In: CLAWAR, pp. 505–516 (2003)
14. Kajita, S., Kanehiro, F., Kaneko, K., Yokoi, K., Hirukawa, H.: The 3D linear inverted pendulum mode: a simple modeling for a biped walking pattern generation. IEEE/RSJ IROS 1, 239–246 (2001)
15. Nise, N.S.: Control systems engineering, 4th edn. John Wiley and Sons, USA (2004)
16. Slotine, J.J.E., Li, W.: Applied nonlinear control. Printice-Hall international editions, London (1991)
17. Napoleon, N.S., Sampei, M.: Balance control analysis of humanoid robot based on ZMP feedback control. IEEE/RSJ IROS 3, 2437–2442 (2002)
18. Okumura, Y., Tawara, T., Endo, K., Furuta, T., Shimizu, M.: Realtime ZMP compensation for biped walking robot using adaptive inertia force control. In: IROS, vol. 1, pp. 335–339 (2003)
19. Katayama, T., Ohki, T., Inoue, T., Kato, T.: Design of an optimal controller for a discrete-time system subject to previewable demand. Int. J. of Control 41(3), 677–699 (1985)